



On the stability of composite plate shear walls under fire loading

Saahastaranshu R. Bhardwaj¹, Shivam Sharma², Ataollah T. Anvari³, Amit H. Varma⁴

Abstract

Composite plate shear walls (C-PSWs) are being considered for commercial building construction due to their benefits of modularization and schedule contraction. Fire hazard is an important consideration for building design, and the applicability evaluation of the C-PSW system for buildings would be incomplete without consideration of fire loads. The existence of steel plates (analogous to reinforcing bars in traditional reinforced concrete construction) on the surface of the shear walls means that the steel plates will be directly exposed to fire temperatures. Fire loading will result in elevated steel and concrete temperatures and non-linear thermal gradients through the cross-section of the walls. Elevated temperatures result in the degradation of the mechanical properties of steel and concrete. This can result in local buckling of steel plates or global instability of the walls, leading to the collapse of the walls at gravity load magnitudes significantly lower than the ambient compression strength of the walls. The authors have initiated a research project focusing on stability of C-PSWs under fire loading. The existing standard fire tests conducted on scaled C-PSW specimens in S. Korea and China are summarized in the paper. This paper focuses on the development of detailed finite element models to evaluate the stability response of C-PSWs under fire loading. The existing experimental database has been used to benchmark finite element models for the thermal and structural response of the system. The numerical models are conservative in comparison to the experimental results. The surface temperature at failure is a better indicator of the fire resistance of the C-PSWs (in comparison to time to failure). The time to failure can be determined from the surface temperature at failure. The benchmarked analyses will be employed to develop full-scale models of C-PSWs. Parametric studies will be conducted to study the effect of variation in section thickness, steel reinforcement ratio, steel plate slenderness on the local and global stability behavior of C-PSWs subjected to standard fire curves. The authors will also be conducting a series of experimental studies where C-PSW specimens will be subjected to standard fire curves. Results of experimental and numerical studies will be employed to determine the fire resistance of C-PSWs, obtain fire ratings for walls, and provide detailing or design recommendation for performance-based fire design of C-PSWs. These recommendations will enable the engineers to consider fire loading in the design of C-PSWs for building structures.

¹ Postdoctoral Researcher, Purdue University, USA, sbhardwa@purdue.edu

² Undergraduate Student, Indian Institute of Technology, Hyderabad, India, ce15btech11021@iith.ac.in

³ Doctoral student, Purdue University, ataghipo@purdue.edu

⁴ Karl H. Kettelhut Professor and Director of Bowen Laboratory, Purdue University, ahvarma@purdue.edu

1. Introduction

Concrete filled composite plate shear walls (C-PSW/CF) are being considered for commercial construction due to the advantages of modularity and schedule construction. The C-PSW/CF system comprises of steel plates sandwiching concrete infill. Steel plates are connected to each other through ties. Ties ensure structural integrity of the system (Seo et al. 2017) and serve as out-of-plane shear reinforcement (Bhardwaj et al. 2017). Composite action between steel plates and concrete infill is provided by shear studs and / or ties. There has been significant research regarding the behavior and design of steel-plate composite walls (analogous to C-PSW/CF) for application in safety-related nuclear facilities. The research and design provisions have been discussed in detail by Bhardwaj and Varma (2017a).

There has been recent research on the commercial building application of C-PSW/CF (Selvarajah 2013, Bruneau et al. 2013, Ji et al. 2013, and Varma et al. 2017). The current building codes, namely ASCE 7 (2016) and AISC 341 (AISC 2016), permit the use of C-PSW/CF, with and without boundary elements, in seismic regions (Bruneau et al. 2013, Alzeni and Bruneau 2014, Epackachi et al. 2015, Kurt et al. 2016, Bhardwaj et al. 2018a). The lateral capacity of C-PSW/CF (for wind and seismic loads) has also been investigated by Wang et al. (2018).

C-PSW/CF need to be designed for the limit state of local buckling of the faceplates (local instability). The local buckling of steel plates depends on the steel plate slenderness, and parameters such as initial imperfections and concrete casting pressure. Bhardwaj and Varma (2016, 2017b) developed a procedure to incorporate the effects of initial imperfections and concrete casting pressure on the compression behavior of C-PSW/CF. Bhardwaj et al. (2018b) also provided recommended steel plate (web plates and flange plate) slenderness criteria for C-PSW/CF. The stability of empty steel C-PSW modules was evaluated by Shafaei et al. (2018a, 2018b).

An important aspect of applicability evaluation of C-PSW/CF for commercial construction is the stability behavior of these walls under fire loading. Steel plates (analogous to reinforcing bars in traditional reinforced concrete construction) form the exterior of C-PSW/CF. The steel will be directly exposed to fire temperatures (in absence of fire protection). Fire loading will result in elevated steel and concrete temperatures and non-linear thermal gradients through the cross-section of the walls. Elevated temperatures will result in degradation of mechanical properties of steel and concrete and may cause instability (local or global) and failure of walls at axial loads significantly lower than the ambient strength of the walls. There is a need to experimentally and numerically evaluate the stability response of C-PSW/CF under fire loading.

The authors have initiated a research project focusing of behavior of C-PSW/CF subjected to axial compressive and fire loading. The stability behavior of C-PSW/CF under fire loading will be evaluated experimentally. Benchmarked numerical models will be developed to conduct parametric studies. The experimental and numerical results will be employed to develop recommendations for prescriptive design of C-PSW/CF under fire loading. Numerical tools will be developed that enable the engineers to perform performance-based design of C-PSW/CF subjected to fire loading.

This paper summarizes the existing experimental studies for C-PSW/CF walls subjected to fire loading. The paper focuses on the development and benchmarking of 2-D and 3-D finite element models for investigating the response of C-PSW/CF. The paper also presents a summary of the proposed experimental and parametric study cases.

2. Summary of existing research

There is limited experimental data on the response of C-PSW/CF subjected to fire loading. Researchers in South Korea have conducted experimental studies for stiffened steel plate concrete walls (with ribs as stiffeners) subjected to fire loading (Moon et al. 2009). Moon et al. subjected 3000 × 3000 × 300 mm wall specimens to ISO 834 fire curve (ISO 1975). However, the specimen steel plates were stiffened with ribs, which potentially improve the stability response of these walls. Axial load ratios of 40% and 63% of the design axial strength were applied in combination with fire loading. The fire resistance rating of specimens with 40% and 63% axial load was 180 minutes and 89 minutes respectively. The specimens failed due to local bulging of surface steel plates, spalling of concrete and stud / tie weld rupture. Kim et al. (2009) evaluated the response of half SC slabs subjected to one-sided fire loading.

Recently, Wei et al. (2017) have investigated the fire resistance of 12 concrete filled steel plate composite wall specimens. The authors subjected the specimens to combined gravity and fire loading. The tests were conducted in a gas furnace with the air temperature controlled to match the ISO 834 fire curve. Specimens 1 to 8 were subjected to uniform fire and specimens 9 to 12 were subjected to one-sided fire. The specimens had a width of 1000 mm. The parameters varied included (a) height: 850, 1000, 1350 and 1850 mm, (b) thickness: 150 and 200 mm, (c) steel plate thickness: 2 to 5 mm, and (d) fire loading: uniform and one-sided fires. The axial load ratio was maintained around 30%. Specimens subjected to uniform fires failed due to local buckling, or weld cracking. The fire resistance times were higher than 2 hours for all the specimens. The specimen with 200 mm concrete thickness had a failure time of 212 minutes. The tallest specimen (1850 mm height) failed due to global instability. Specimens subjected to single-sided fires underwent thermal insulation failure, with the earliest failure time being 166 minutes. No specimen failure was observed for one-sided fires. The specimen with thickness of 200 mm did not undergo insulation failure till the test was stopped (207 minutes). Experimental studies by Wei et al. present significant data for development of benchmarked models for parametric numerical studies.

3. Benchmark numerical models

The Finite Element Method (FEM) is employed to numerically examine the behavior of C-PSWs under a combination of fire and gravity loads. The FEM models are developed and benchmarked to the experimental studies conducted by Wei et al. (2017). Two-dimensional and three-dimensional finite elements models of the specimens tested by Wei et al. (2017) were developed in a commercially available software, ABAQUS (Simulia 2016). Two-dimensional modeling was employed to evaluate the fundamental thermal behavior of the C-PSWs when subjected to fire, i.e., the evolution of through thickness temperatures. Three-dimensional models were developed to evaluate the stability response of C-PSWs under gravity and fire loading. The numerical studies provided insights into the material and structural level response of walls subjected to fire loading. The numerical results were compared with experimental results.

3.1 2-D Models

Two-dimensional finite element models of walls were developed to obtain evolution of through thickness temperatures in the wall. The wall assembly consists of a concrete mid- and side-blocks, which are enclosed by steel plates (consistent with specimens tested by Wei et al. 2017). All the components of the assembly are modeled using DC2D4 element type, which is a 2-D, 4-node quadrilateral, heat transfer element. The thermal properties of steel and concrete are defined as per the Eurocode (2005) and are discussed in detail in section 3.3. Fig. 1 shows the plan view of the specimen modeled for this study. The outer layer shows the steel plates enclosing the concrete blocks.

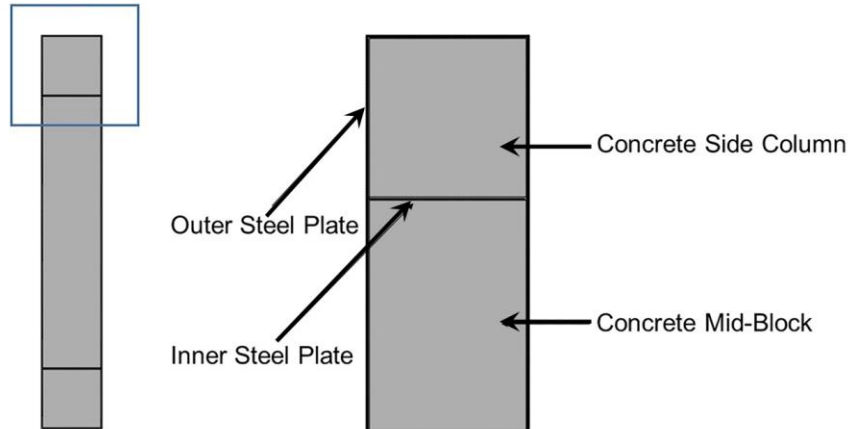


Figure 1. 2-Dimensional Model showing different components

3.2 3-D Models

Three-dimensional models are developed to evaluate the behavior of CFSWs when subjected to fire and gravity loads. The details of the specimens tested by Wei et al. (2017) were modeled, including the studs and tie bars. The 3-D view of the model is shown in Fig. 2. The concrete block is modeled using 3-D solid elements whereas the steel flange, web and inner plates are modeled as shell elements. Since the thickness of steel plates is diminutive as compared to the thickness of the concrete block, shell elements are preferred for modeling steel plates. Additionally, sequentially coupled thermal-stress analysis is computationally expensive and the use of shell elements makes the analysis computationally efficient. The shear studs and ties are both modeled as beam elements. The thermal properties and mechanical properties of all the materials for 3-D models are consistent with those for 2-D Models.

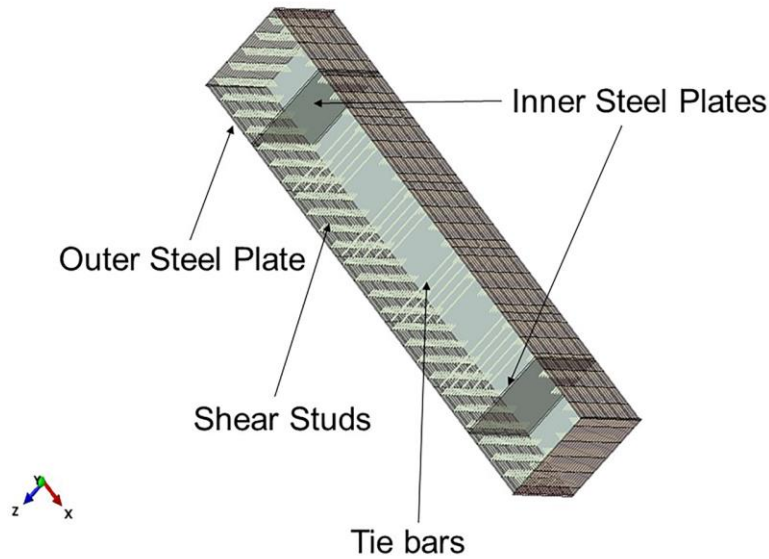


Figure 2. 3-Dimensional model of the CFSP walls (as tested by Wei et al. 2017)

3.3 Thermal and mechanical properties

The thermal properties of steel and concrete are defined as per the Eurocode (2005). The moisture content is considered to be 3% (based on calibration studies for heat transfer results), and the specific heat is chosen accordingly. The upper limit values of thermal conductivity specified by the Eurocode are used for concrete. The thermal expansion values of siliceous aggregate concrete are used.

The mechanical properties of steel and concrete are also defined per the Eurocode. The load-deformation response of a member varies significantly with temperature and needs to be taken into account while defining the mechanical properties. Fig. 3(a) and Fig. 3(b) show the temperature dependent stress-strain curves for concrete (having a cylinder strength of 50 MPa) and steel (having a yield strength of 500 MPa) respectively. Concrete material behavior was modeled using ‘Concrete damaged plasticity’ model in ABAQUS. The steel material was modeled as ‘elastic-plastic’.

3.4 Sequentially coupled analysis

ABAQUS provides different options for conducting thermal-stress analysis. Sequentially coupled thermal-stress analysis technique was employed for this study. The technique involves conducting heat-transfer analysis for the models. The nodal temperatures from heat-transfer analysis serve as inputs for the stress analysis model.

Heat transfer analysis

The model consisted of concrete blocks and the steel assembly (as shown in Fig. 2). The concrete is modeled using DC3D8 element, which is an 8-node linear heat transfer brick element, and the steel plates are modeled using DS4 element. The steel plates are tied to the outer surface of the concrete block to facilitate heat transfer between steel and concrete. The inner plates are also tied to the concrete block. This approach is conservative as it does not consider the energy loss at steel-concrete interface and may result in cross-section temperatures marginally higher than those observed experimentally. The ambient temperature is assumed to be 20 °C and the specimens are

subjected to ISO-834 standard fire curve for 4 hours. The heat flow between the burning gases and the steel surface is simulated using the ‘FILM’ subroutine in ABAQUS. This subroutine provides the temperatures at the outer surface of the specimen (the surface exposed to fire) by accounting for the radiation and convection modes of heat transfer between the surface and the gas temperatures. For brevity, the details of this subroutine are not discussed here and are reported by Cedeno et al. (2009).

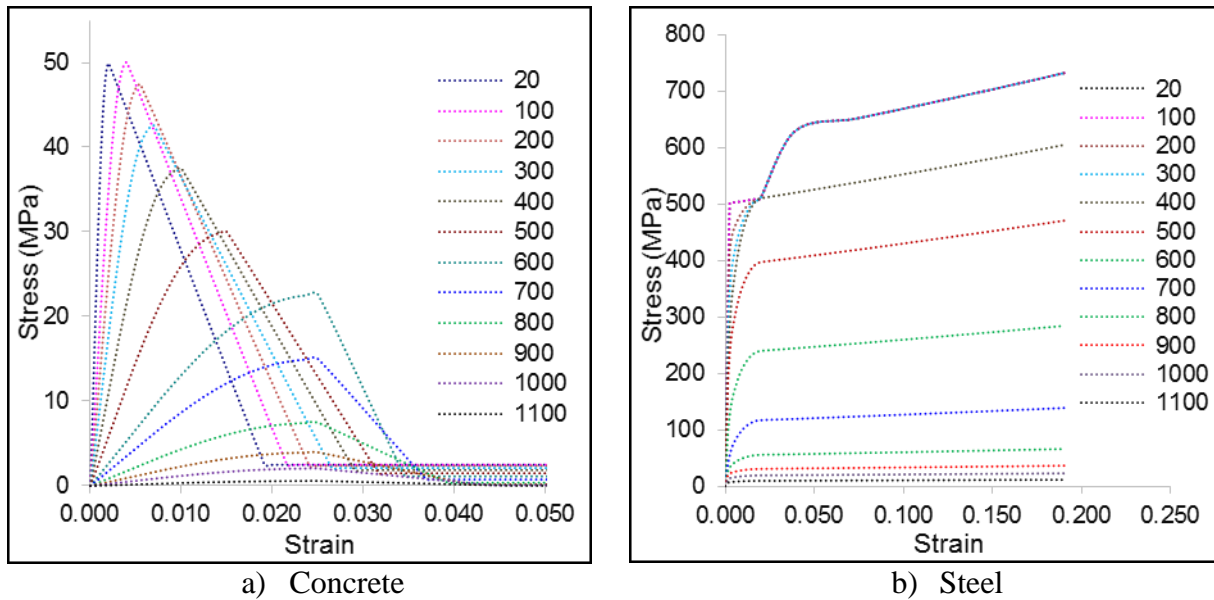


Figure 3. Stress-strain curves at elevated temperatures ($^{\circ}\text{C}$) for (a) concrete with $f'_c=50$ MPa and (b) steel with $f_y=500$ MPa

Stress analysis

The stress analysis model is consistent with the heat transfer model. Additionally, the stress model includes the shear studs and tie bars. The concrete is modeled using C3D8R element, an 8-node linear brick element with reduced integration. The steel plates are modeled using S4R element, a 4-node general-purpose linear shell element. These reduced integration elements are used to increase the computational efficiency of the analysis. The shear studs and the tie bars are modeled using B31 element, a 2-node linear beam element. Fire analysis may result in failure of stud /tie welds (as observed by Wei et al. 2017). Therefore, cartesian type connector elements were employed to simulate the temperature dependent force-slip behavior of studs and ties. The force-slip relationship for the connectors was based on Ollgaard et al. (1971) and was modified to consider temperature dependent properties as discussed by Selden (2014).

The C-PSW specimens have all the degrees of freedom restrained at the bottom surface. Gravity loading is applied on the top surface. The tie bars and shear studs are embedded in the concrete block. The ambient temperature of the specimen is taken as 20°C and the temperatures at any other time are interpolated from the nodal temperatures from heat transfer analysis (serve as input for stress analysis). A hard and frictionless contact is defined between different components of the assembly. The stress analysis is a 2-step process. In the first step, an incremental axial compressive load is applied on the specimen (magnitude increased from zero to the maximum value in 1 hr). In

the second step, the axial load is maintained constant, and nodal temperatures based on the heat transfer analysis are applied. The second step continued for 4 hours. The run times for thermal and stress analyses are scaled down by accordingly scaling up the thermal conductivity of steel and concrete.

4. Comparison of numerical and experimental results

The numerical models were employed to obtain stability response of the specimens tested by Wei et al. (2017). This section compares the results of thermal and stress analysis with experimental results. For brevity, thermal and stress analysis for only three specimens [2 uniform fire specimens (SCW6 and SCW 7) and 1 one-sided fire specimen (SCW12)] are discussed. The summary of the results for the three specimens (as presented in Table 1) is then described.

4.1 Thermal analysis

Heat transfer analyses were conducted for specimens following the procedure discussed previously in Section 3. The typical through thickness temperature distributions (in °C) for uniform fire and one-sided fire conditions are shown in Fig. 4(a) and Fig. 4(b) respectively. The figure shows temperature profiles at 4 hours after the fire event. Uniform fire results in rise of steel temperature (up to 1100 °C), with the concrete infill at 750 °C. One-sided fires result in surface temperature increase on the exposed (heated) side. There is a thermal gradient through the cross-section with the unexposed side temperature close to 280 °C.

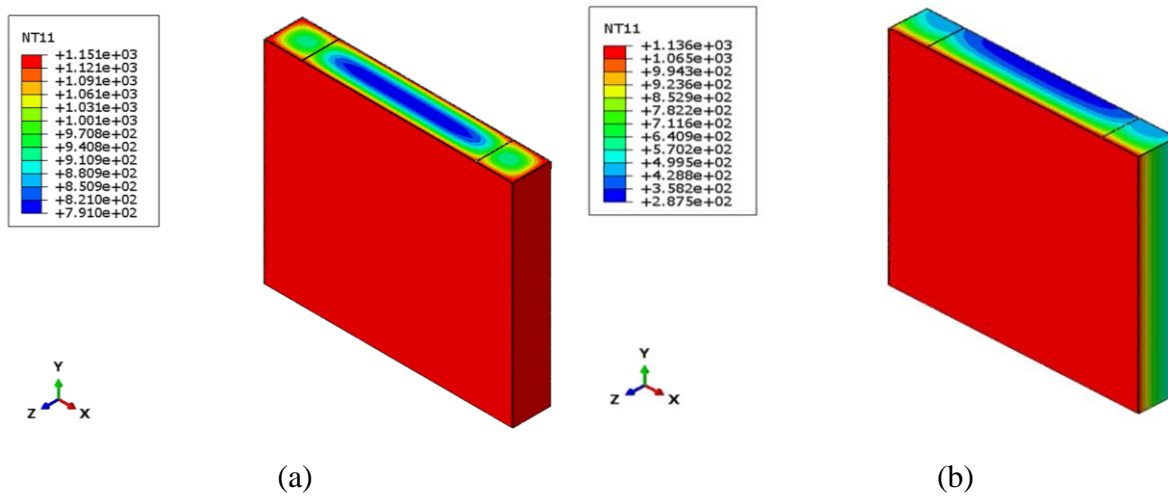


Figure 4. Temperature Distribution for (a) Uniform fire and (b) One-sided fire conditions (at 3 hours after the fire event)

Figure 5 presents the comparison of temperature profiles obtained numerically with those observed experimentally (for SCW6, 7 and 12). The numerically observed mid-thickness temperature for uniform fire specimens (SCW 6 and 7) and unexposed-side temperature for single-sided fire specimen (SCW 12) compare well with experimental results. However, the outer surface temperature or exposed-side temperature values obtained from FE models are higher than the experimental values in some regions of the curve.

The experimentally observed surface temperatures indicate a plateau in the first 30 minutes of the heating. Wei et al. (2017) attribute this to the latent heat associated with the loss of moisture

content from the concrete infill. To investigate this, concrete specific heat values corresponding to different moisture content were used in the FE models. However, no significant difference in the surface temperature evolutions was observed. The change in moisture content affected the evolution of temperature at mid-thickness of the cross-section. The plateau observed in experimental measurements could be due to some heat loss or inconsistencies in the measurements. The experimental surface temperatures are reported at 2 mm from the concrete surface. The steel surface temperatures are not reported. The plateau observed after 30 minutes may be due to an air gap between steel and concrete as the plate buckling initiates. Additionally, the FE models incorporate thermal ties (no heat loss at interface) at steel concrete interface. This may conservatively result in higher surface temperatures in the FE models. The higher surface temperatures in FE models will result in higher heat flux input for FE models (in comparison to experiments) and may reduce the time to failure of the specimens.

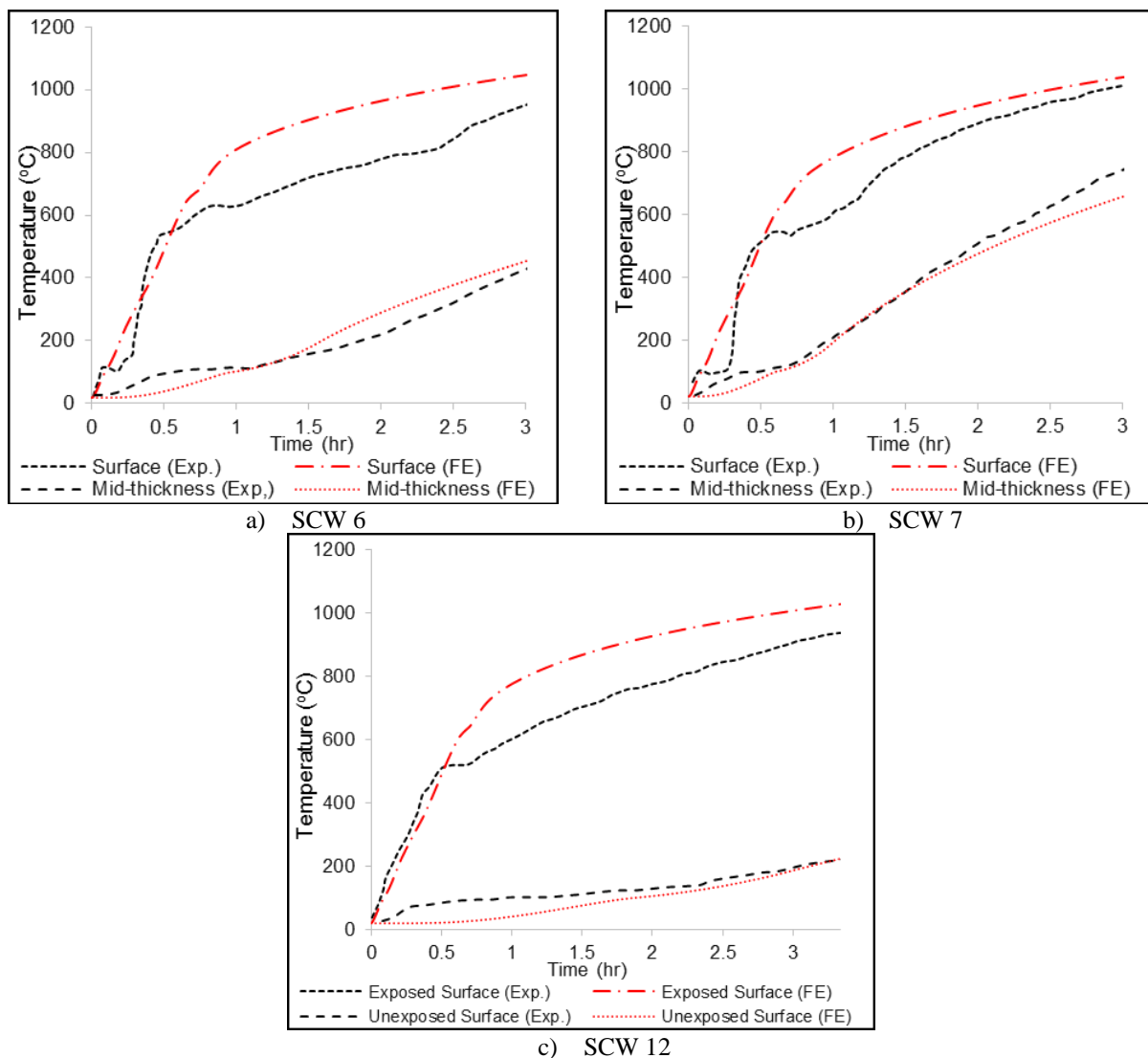
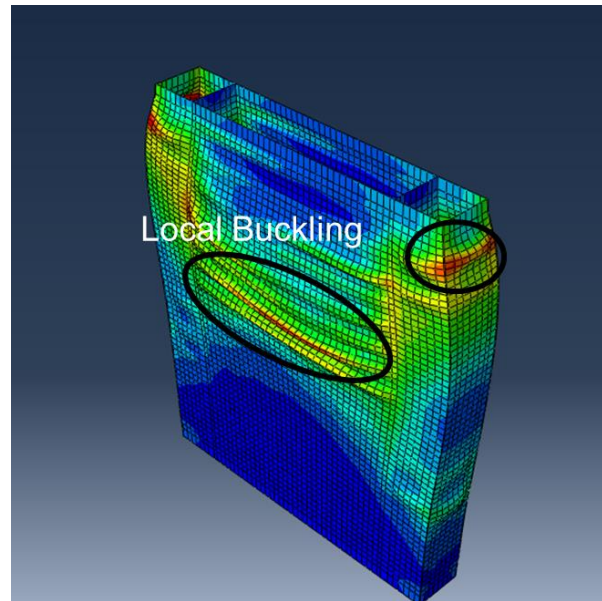


Figure 5. Comparison of predicted temperatures from the Finite Element (FE) analysis with the experimental (Exp.) data at different sections

4.2 Stress analysis

Wei et al. (2017) observed that fire loading resulted in failure of the specimens due to local buckling of the steel plates, weld cracking, and concrete crushing. Fig. 6 compares the specimen state at failure for uniform fire loading. Consistent with experimental observations (Fig. 6a), FE model exhibited extensive buckling of the steel plates (both web and flange) at failure. The axial deformation response of the FE models can be compared with experimental results. Fig. 7 and 8 present the axial deformation with time for the specimens. The axial deformation curves for experiments have been corrected for some inconsistencies in the measurements (e.g., loss of axial loading in SCW 6, and an offset in the initial axial deformation). In the initial stages (up to 30 minutes), the uniform-fire specimens (Fig. 7) underwent a thermal expansion. This was followed by a stage of axial compression, which lasted for next 60 minutes. As the steel and concrete temperatures increase, resulting in degradation of material strengths, the axial compressive deformation overcomes thermal expansion. The axial compression increased gradually, and finally the specimen failed undergoing rapid axial shortening. Similar behavior was observed on the exposed side of the one-sided fire specimen (Fig. 8a). However, the unexposed side kept on expanding throughout the fire, before specimen failure (Fig. 8b).



a) Experiment

b) FE model

Figure 6. Specimen state at failure (uniform fire loading)

Axial deformation vs time response obtained from FE models compares reasonably with that observed experimentally (Fig. 7 and 8). However, the FE failure time is lower than experimental failure times. This may be because of higher surface temperatures for FE models (as discussed previously) or some variability in the recorded experimental measurements. To investigate this further, the axial displacements of the specimens were plotted against the surface temperature (Fig. 9 and 10). The FE model surface temperature at failure agrees well with experimentally observed surface temperature at failure. Therefore, surface temperature may be a better indicator of specimen failure for FE models. The failure time can then be calculated using heat transfer equations and surface temperatures.

A summarized comparison of experimental and finite element results for SCW 6, 7 and 12 is presented for specimens in Table 1. The table presents the parameters varied in the specimens, and the experimental and numerical failure times and surface temperatures at failure. The failure times obtained from FE analyses are conservative with respect to experimental failure times. FE analyses directly using experimental surface temperature data (instead of ISO fire curve inputs) were also conducted for these specimens. These analyses resulted in a failure time that was closer to experimental observations. However, considering potential variability in experimental observations, using the ISO fire curve is a more reliable and conservative approach to determine the failure time and surface temperature for C-PSWs. Table 1 indicates that the experimentally observed surface temperature at failure is in better agreement with the numerical results (in comparison to failure times). Therefore, the surface temperature at failure is recommended to be used to determine the fire resistance of C-PSWs. Some further improvements may be possible by defining the thermal contact at steel-concrete interface. However, the FE models are expected to be conservative in comparison to experimental results due to inherent limitations of the material stress-strain curves at extreme temperatures.

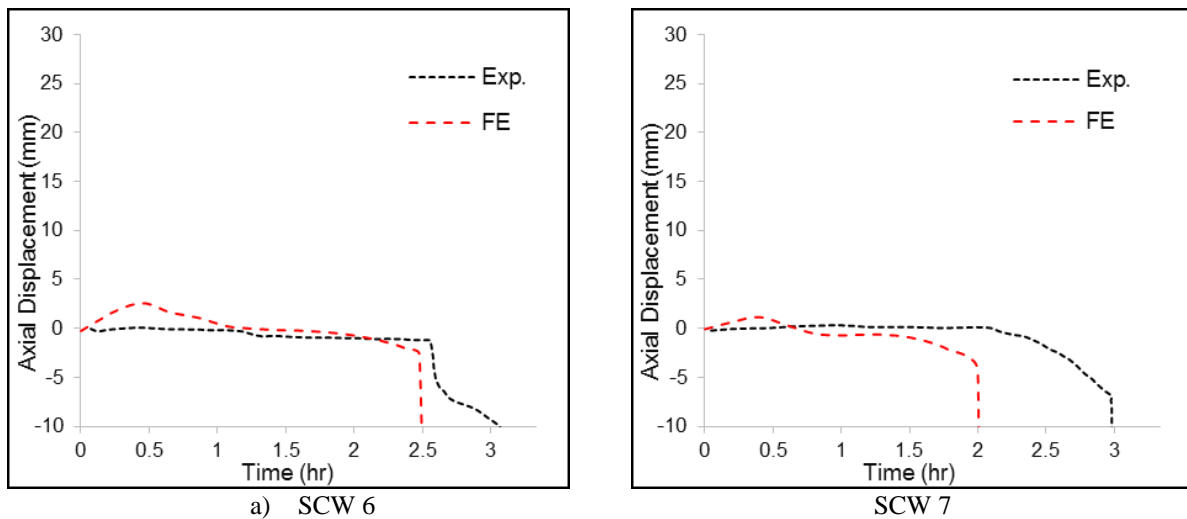


Figure 7. Comparison of axial displacement obtained from the Finite Element (FE) analysis with the experimental (Exp.) data.

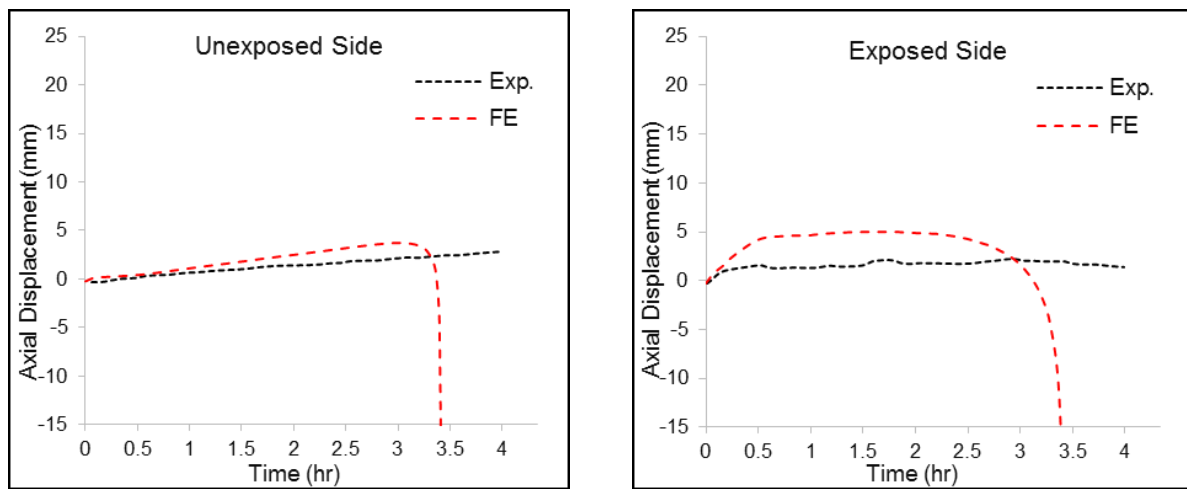


Figure 8. Comparison of axial displacement for SCW 12 obtained from the Finite Element (FE) analysis with the experimental (Exp.) data at (a) Unexposed Side (b) Exposed Side

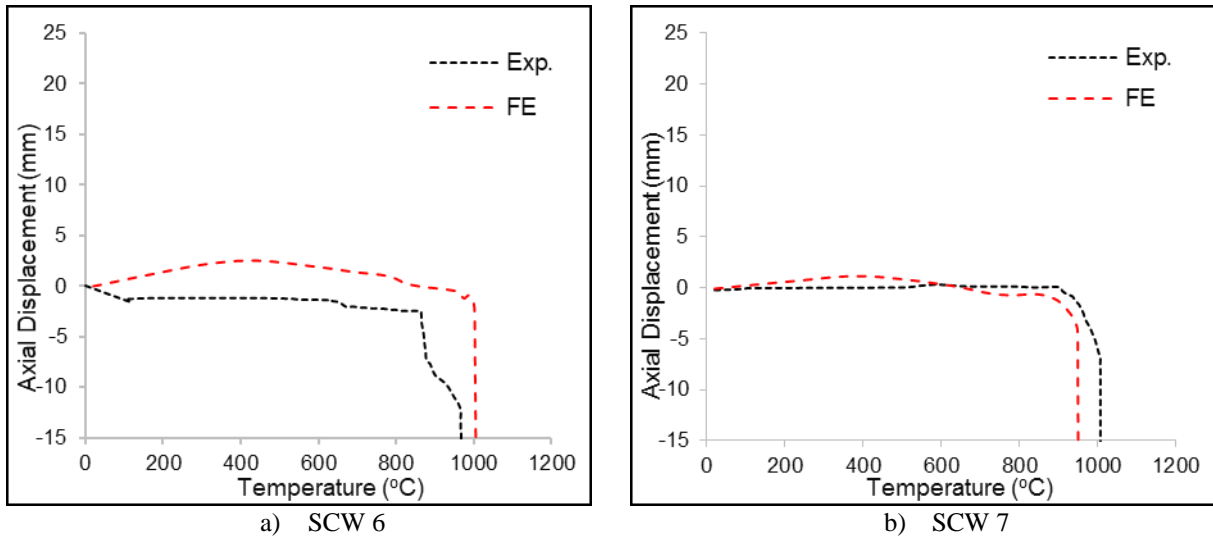


Figure 9. Comparison of axial displacement v/s outer surface temperatures obtained from the Finite Element (FE) analysis with the experimental (Exp.) data

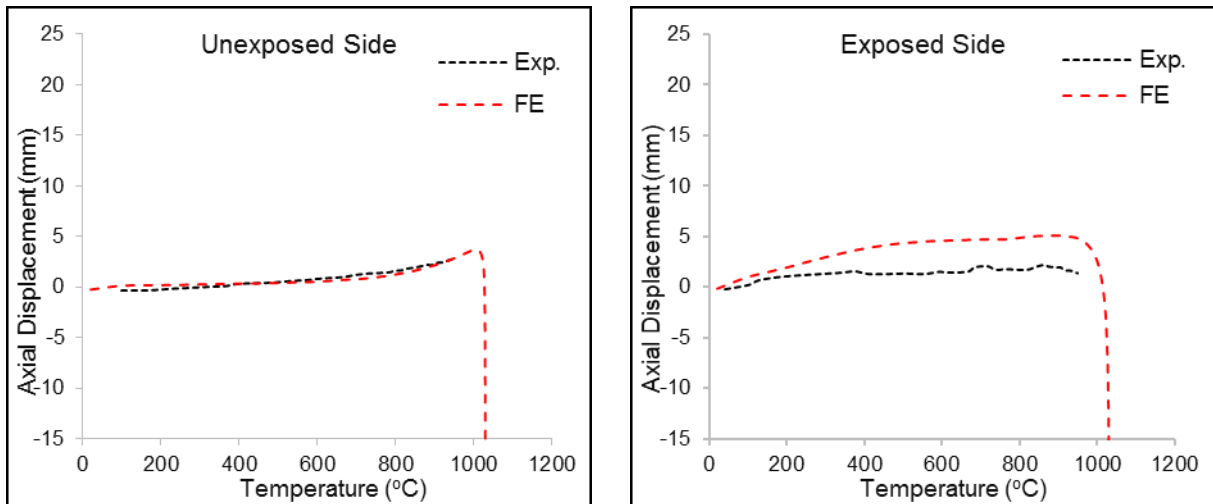


Figure 10. Comparison of axial displacement v/s outer surface temperatures experienced by the SCW 12 obtained from the Finite Element (FE) analysis with the experimental (Exp.) data at (a) Unexposed Side (b) Exposed Side

Table 1. Summary of Finite Element and Experimental Results (specimens tested by Wei et al. 2017)

Fire Scenario	Specimens	Height (H)	Wall thickness (T)	Steel plate thickness (t)	Shear studs	Tie bars	Load Ratio (d)	Exp. Failure Time (min)	FE Failure Time (min)	Exp. Failure Surface Temp. (C)	FE Failure Surface Temp. (C)
Uniform Fire	SCW6	850	200	4	Φ2@40	Φ10@160	0.34	212	150	870	1000
	SCW7	850	150	2	Φ2@40	Φ10@160	0.4	178	120	930	950
One-sided Fire	SCW12	1000	150	3	Φ2@40	No tie bars	0.34	166	196	950	1015

All dimensions in mm, unless noted otherwise.

5. Future work

The authors are currently conducting experimental studies to investigate the stability response of C-PSWs with different configurations. C-PSW specimens will be subjected to a combination of gravity and fire loading. Fire loading will be applied using radiant ceramic fiber heaters. The parameters considered in the experiments will be tie diameter and spacing, magnitude of axial load, uniform and one-sided heating, steel reinforcement ratio, and specimen height. The results from these experiments will be evaluated and additional specimens may be tested to consider the effect of a wider range of parameters. Benchmarked numerical models of the specimens tested by authors will also be developed to gain deeper insight into the behavior of C-PSWs for fire loading. Additional studies will be conducted to investigate the effect of parameters not considered in the experiments. The results from experimental and numerical studies will be employed to develop design recommendations for fire loading. Additionally, numerical tools will be developed for performance-based design of C-PSWs.

6. Summary and conclusions

C-PSWs are being employed in high-rise building construction. The stability response of these walls under fire loading needs to be investigated. This paper presents the development of detailed finite element models to numerically investigate the behavior of C-PSWs under gravity and fire loading. The numerical models have been benchmarked with existing experimental data. The finite element models conservatively estimate the response of experiments. The fire resistance time of C-PSWs increases with increase in section thickness. However, the fire resistance time decreases with increase in specimen height. Due to potential variability associated with experimental data, the conservative failure time and surface temperature estimates from the finite element models are the preferred option to determine the fire resistance of C-PSWs. The surface temperature at failure of finite element models matches closely with the surface temperatures of specimens at failure (in comparison to time to failure). Therefore, it is recommended to use the surface temperature at failure as a metric to determine the fire resistance of C-PSWs. The time to failure can then be calculated using the section properties and heat transfer equations.

The paper also presents a discussion on the experiments that are being conducted by the authors. The benchmarked numerical models will be employed to conduct parametric studies for C-PSWs. The results from experimental and numerical studies will form the basis for detailing and design recommendations for C-PSWs subjected to fire loading. The results will also be used to benchmark and validate numerical tools for performance-based design of C-PSWs.

7. References

- AISC (2016). *Seismic Provisions for Structural Steel Buildings*. AISC 341, American Institute of Steel Construction, Chicago, IL.
- Alzeni, Y. and Bruneau, M. (2014), "Cyclic Inelastic Behavior of Concrete Filled Sandwich Panel Walls Subjected to In-Plane Flexure," *Technical Report MCEER-14-0009*, MCEER, University at Buffalo, Buffalo, NY.
- ASCE (2016). *Minimum Design Loads for Buildings and Other Structures*, American Society of Civil Engineers, ASCE 7. Reston, VA, 2016.
- Bhardwaj, S.R., and Varma, A.H. (2016). "Effect of Imperfections on the Compression Behavior of SC Walls." *Proceedings of the Annual Stability Conference*, Structural Stability Research Council, Orlando, FL. April 12-15, 11 pp
- Bhardwaj, S.R., and Varma, A.H. (2017a). "Design of Modular Steel-plate Composite Walls for Safety-related Nuclear Facilities." *AISC Design Guide 32*. American Institute of Steel Construction, Chicago, IL, USA.

- Bhardwaj, S.R., and Varma, A.H. (2017). "SC Wall Compression Behavior: Interaction of Design and Construction Parameters." *Proceedings of the Annual Stability Conference*, Structural Stability Research Council, San Antonio, Texas, March 2017, 14 pp.
- Bhardwaj, S.R., Varma, A.H., Orbovic, N. (2018a). "Behavior of Steel-plate Composite Wall Piers under Biaxial Loading," *Journal of Structural Engineering*, ASCE, Vol. 145, Issue 2, Feb. 2019. [https://doi.org/10.1061/\(ASCE\)ST.1943-541X.0002247](https://doi.org/10.1061/(ASCE)ST.1943-541X.0002247)
- Bhardwaj, S.R., Wang, A.Y., Varma, A.H. (2018b), "Slenderness Requirements for CF-CPSW: The Effects of Concrete Casting," in *Proceedings of Eighth International Conference on Thin-Walled Structures*, Lisbon, Portugal, 15 pp
- Bruneau, M., Alzeni, Y., and Fouché, P. (2013). "Seismic behavior of concrete-filled steel sandwich walls and concrete-filled steel tube columns" *Steel Innovations 2013 Conf.*, Christchurch, New Zealand.
- Cedeno, G., Varma, A.H., and Agarwal, A. (2009). "Behavior of Floor Systems under Realistic Fire Loading," *Proceedings of the 2009 Structures Congress*, ASCE.
- Eurocode (2005). "Eurocode 4: Design of Composite Steel and Concrete Structures—Part 1-2: General Rules Structural Fire Design", EN 1994-1-2, Brussels, Belgium.
- Epackachi, S., Nguyen, N., Kurt, E., Whittaker, A. and Varma, A.H. (2015), "In-Plane Seismic Behavior of Rectangular Steel-Plate Composite Wall Piers," *Journal of Structural Engineering*, ASCE, Vol. 141, No. 7.
- Feng, Wei., Cheng, Fang., Bo, Wu., (2017). "Fire resistance of concrete-filled steel plate composite (CFSPC) walls." *Fire Safety Journal*, 88, 26-39.
- ISO-834 Fire resistance tests-elements-elements of building construction. *International Standard ISO 834*, Geneva, 1975.
- Ji, X., Cheng, X., Jia, X., and Varma, A.H. (2017). "Cyclic In-Plane Shear Behavior of Double-Skin Composite Walls in High-Rise Buildings." *Journal of Structural Engineering*, Vol. 143, No. 6, ASCE, Reston, VA. [https://doi.org/10.1061/\(ASCE\)ST.1943-541X.0001749](https://doi.org/10.1061/(ASCE)ST.1943-541X.0001749)
- Kim, W., Jee, N., Lee, C.S., Mun, T.Y. (2009). "Performance-based Fire Design of Half SC Slabs in Nuclear Power Plants." *Transactions of International Conference on Structural Mechanics in Reactor Technology, SMiRT 20*, Div. 6, Paper 1698, Espoo, Finland
- Kurt, E.G., Varma, A.H., Booth, P.N. and Whittaker, A. (2016), "In-plane Behavior and Design of Rectangular SC Wall Piers Without Boundary Elements," *Journal of Structural Engineering*, ASCE, Vol. 142, No. 6.
- Moon, I, Jee, N, Kim, W, Lee, C.S., Yoo, S.T. (2009). "Performance-based design of Stiffened Steel Plate Concrete Wall in Fire,". *Transactions of International Conference on Structural Mechanics in Reactor Technology, SMiRT 20*, Div. 6, Paper 1675, Espoo, Finland.
- Ollgaard, J. G., Slutter, R. G., & Fisher, J. W. (1971). "Shear strength of stud connectors in lightweight and normal weight concrete." *AISC Eng'g Jr.*, April 1971 (71-10).
- Selden, K. L. (2014). "Structural behavior and design of composite beams subjected to fire." Ph.D. dissertation, Purdue Univ., West Lafayette, IN.
- Selvarajah, R. (2013). "Behavior and design of earthquake-resistant dualplate composite shear wall systems." Ph.D. dissertation, Purdue Univ., West Lafayette, IN.
- Seo, J., Varma, A. H., Sener, K., & Ayhan, D. (2016). "Steel-plate composite (SC) walls: In-plane shear behavior, database, and design." *Journal of Constructional Steel Research*, 119, 202-215.
- Shafaei S., Wang A., Varma A.H., and Morgen B. (2018a). "Stability of Steel Modules during Construction." *Proceedings of the Annual Stability Conference-Structural Stability Research Council*. Baltimore, Maryland, April 10-13, 2018
- Shafaei S., Wang A., Varma A.H., and Morgen B. (2018b). "Shear Buckling of Thin-Walled Built-Up Steel Modules Before Composite Phase." *Eighth International Conference on Thin-Walled Structures-ICTWS*, Lisbon, Portugal, July 24-27, 2018
- Simulia (2016). *ABAQUS 2017 Documentation*, Dassault Systemes Simulia Corporation Providence, RI.
- Varma, A.H., Lai, Z., and Seo, J. (2017). "An Introduction to coupled composite core wall systems for high-rise construction." *Proceedings of the 8th International Conference on Composite Construction in Steel and Concrete*, Wyoming, USA.
- Wang A., Seo J., Shafaei S., Varma A.H., and Klemencic, R. (2018). "On the Seismic Behavior of Concrete-Filled Composite Plate Shear Walls." *Eleventh U.S. National Conference on Earthquake Engineering*. Los Angeles, California, June 25-29, 2018.
- Wei, F., Fang, C., & Wu, B. (2017). "Fire resistance of concrete-filled steel plate composite (CFSPC) walls." *Fire Safety Journal*, 88, 26-39.